Nanotechnology for Environmental Engineering
https://doi.org/10.1007/s41204-021-00180-7

ORIGINAL PAPER

# Comparative studies for the degradation of Reactive Black 5 dye employing ozone-based AOPs

**Sandip Sharma**[1] · **Nikita P. Chokshi**[1] · **Jayesh P. Ruparelia**[1]

Received: 30 July 2021 / Accepted: 25 October 2021

## Abstract

Advanced oxidation processes (AOPs) gain attention for wastewater treatment due to the formation of hydroxyl radicals, which have more oxidation potential. Among all AOPs, few $O_3$, $O_3$/UV, $O_3$/UV/persulfate (PS), and $O_3$/catalyst processes were studied to degrade RB5 dye wastewater. Furthermore, the effect of various experimental parameters like ozone flowrate (30–60 LPH), initial pH (2–12), initial dye concentration (100–1000 mg/L), UV intensity (11–66 W), persulfate dosage, and catalyst dosage (0.5–1.2 g/L) was studied for degradation of RB5. Furthermore, the prepared catalyst was characterized by X-ray diffraction, scanning electron microscopy, energy-dispersive spectroscopy, and BET surface area. Based on the results obtained in the study, the maximum TOC removal efficiency was 96% achieved with optimum operating parameters, 60 LPH of ozone flowrate, 7 pH, 100 mg/L RB5 concentration, and 1 g/L catalyst dosage in 80 min of reaction time using $O_3$/catalyst process, while in $O_3$/UV/PS process, the total organic carbon (TOC) removal efficiency was 90% with optimum operating parameters, 60 LPH of ozone flowrate, 12 pH, 100 mg/L RB5 concentration, UV intensity 66 W, and TOC/PS ratio 1:40 in 80 min of reaction time. Finally, it can be seen that ozone-based AOPs offered an effective solution for the degradation of recalcitrant pollutants, especially RB5.

**Keywords** Dye destruction · Persulfate · Nanocatalysts

## Introduction

Water pollution is the biggest issue being faced by humanity in this era. Availability of fresh and unpolluted water is a primary social and economic concern due to the rapid growth of industry and population worldwide. However, the fast growth in industrialization reflected a rise in pollution in water, air, and soil; simultaneously, the freshwater shortage increased. Therefore, investigation of new treatment technologies that treat the complete removal of pollutants is vital [1]. Advanced oxidation processes (AOPs) such as photocatalysis and ozonation have been studied widely as preferred options for removing pollutants from wastewater [2–12]. Several ozone-based AOPs applied in different types of wastewater treatment are summarized in Fig. 1.

Ozonation is the competent treatment for textile wastewater decomposing many substances, including dyes. The effectiveness of the ozonation process is influenced by better ozone dispersion, intimate contact between the liquid gas phases, and ozone bubble size in the process [1]. However, the ozonation process has some drawbacks that restrict its effectiveness due to its low selectivity and partial oxidation of organic matter; therefore, complete mineralization of the pollutants is not attained [44, 45]. Apart from these limitations, ozone production has relatively low efficiency and high electric energy consumption, so the combination of these processes is extensively studied [13, 14].

$O_3$/UV is a proficient method for degradation of recalcitrant organic pollutants by applying ozonation with UV radiation process for accelerated production of •OH radicals [15]. Complex molecules can be degraded proficiently using combined techniques due to the existence of different reaction pathways. Organic compounds in water may be degraded through a series of oxidation and radical reactions by $O_3$ and •OH radicals. These can be enhanced in the presence of UV radiation. In recent times, recalcitrant organic pollutants are oxidized by persulfate ($S_2O_8^{2-}$) as it has relatively higher oxidation potential ($E^0 = 2.01$) and is most effective for different types of wastewater [16–18, 46].

---

✉ Jayesh P. Ruparelia
jr@nirmauni.ac.in

[1] Chemical Engineering Department, Institute of Technology, Nirma University, Ahmedabad 382481, India

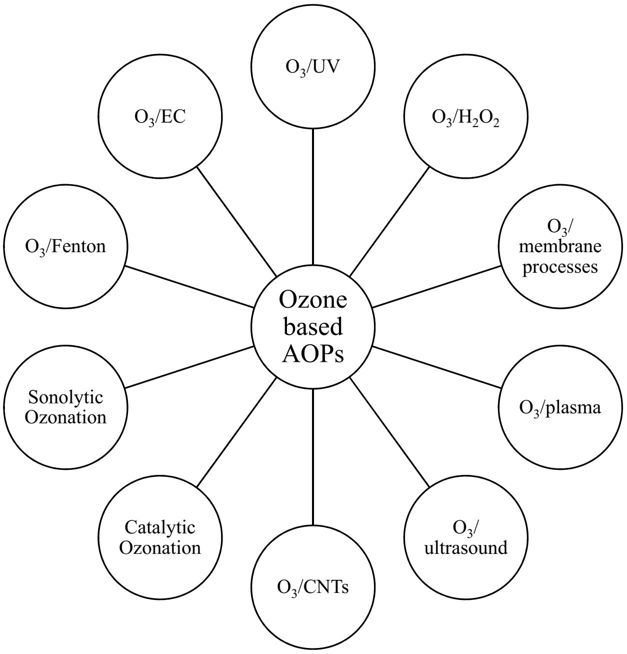

**Fig. 1** Ozone-based AOPs for wastewater treatment

On the other hand, $SO_4^{\bullet-}$ is effective for the degradation of anthraquinone dye due to the ineffectiveness of •OH. It may be due to sulfate radicals having a higher half-life than •OH, favoring electron transfer. Sulfate radicals may be generated by activation of persulfate using heat, UV radiation, metals, or radiolysis [17, 19–21].

Catalytic ozonation gains attention due to its higher efficiency, fast reaction rate, and no secondary pollutant [22]. Furthermore, the heterogeneous catalyst used in the process helps generate hydroxyl radicals, which can react non-selectively with any organic pollutants and increase the mineralization rate [23]. In the past, different metal oxides, metal/metal oxides on supports, mesoporous materials, etc., are used as a catalyst in catalytic ozonation systems. Recently, composite metal oxides have been used to form the new active sites due to the two metal oxides and improve the catalyst activity [22]. It is reported that the cerium is widely used as a catalyst due to its excellent redox property and oxygen storage capacity [10]. Also, due to the multivalence oxidation state of cobalt, it is widely used as a catalyst. Therefore, in this paper, the composite of cobalt and cerium oxide was prepared for the removal of RB5.

Therefore, the main objective of the present study is to compare the performance of ozone-based AOPs such as Ozone ($O_3$), ozone–ultraviolet ($O_3$/UV), ozone–ultraviolet–persulfate ($O_3$/UV/PS), and catalytic ozonation for degradation of Reactive Black 5 (RB5) dye, conducted under various experimental conditions. The present work focuses on the preparation of cerium and cobalt composite metal oxide Ce–Co–O (30/70 wt %) for the degradation of RB5 dye. The catalyst was characterized by the SEM, XRD, EDS, and BET surface area. Operating parameters like ozone flow rate, catalyst dosage, initial pH, and initial concentration of dye were optimized for higher TOC removal efficiency. In addition, catalyst activity was examined for up to four consecutive cycles. In all the experiments, degradation of RB5 was measured as %TOC removal and represented.

## Material and methods

### Materials

The material and chemicals used in the study are potassium iodide (KI), sulfuric acid (98%), sodium hydroxide (NaOH), sodium persulfate ($Na_2S_2O_8$), cerium nitrate hexahydrate ($Ce(NO_3)_3.6H_2O$), cobalt nitrate hexahydrate ($Co(NO_3)_2.6H_2O$), tert-butyl alcohol (TBA), ethylene glycol ($CH_2OH–CH_2OH$), citric acid ($C_6H_8O_7$), nitric acid ($HNO_3$), tert-butyl alcohol (TBA), cerium nitrate hexahydrate ($Ce(NO_3)_3.6H_2O$), cobalt nitrate hexahydrate ($Co(NO_3)_2.6H_2O$), sodium hydroxide pellet (NaOH) and potassium iodide (KI) and distilled water. All chemicals were used of analytical grade without any further purification. Reactive Black 5 was purchased from a local supplier, Ahmedabad, Gujarat.

### Preparation of catalyst

The composite catalyst Co–Ce–O was prepared by the sol–gel method. First, the required amount of Ce $(NO_3)_3.6H_2O$ and Co $(NO_3)_2.6H_2O$ was dissolved in distilled water. After that, the citric acid was added to the solution by a metal nitrate to the citric acid molar ratio of one. The mixture was stirred continuously, and then the required quantity of ethylene glycol was added dropwise. After the completion of the reaction, the solution is heated in a water bath at 80 °C to evaporate water until the gel formation. After the formation of proper gel, it calcined at 400 °C for 5 h in the muffle furnace.

### Experimental procedure

The experimental setup is shown in Fig. 2. All ozone-based AOPs studies were performed using a Pyrex glass column reactor with 1.5 L volume of the synthetic wastewater equipped with a magnetic stirrer. Ozone was generated using pure oxygen in the ozone generator (Aquazone Solutions, Ahmedabad, India) by corona discharge method and injected through a diffuser at the bottom of the glass reactor. The reactor was filled with 1 L of synthetic dye solution, and dye concentration varied from 100 to 1000 mg/L. The experiments were performed at different pH values between 2

**Fig. 2** Experimental setup

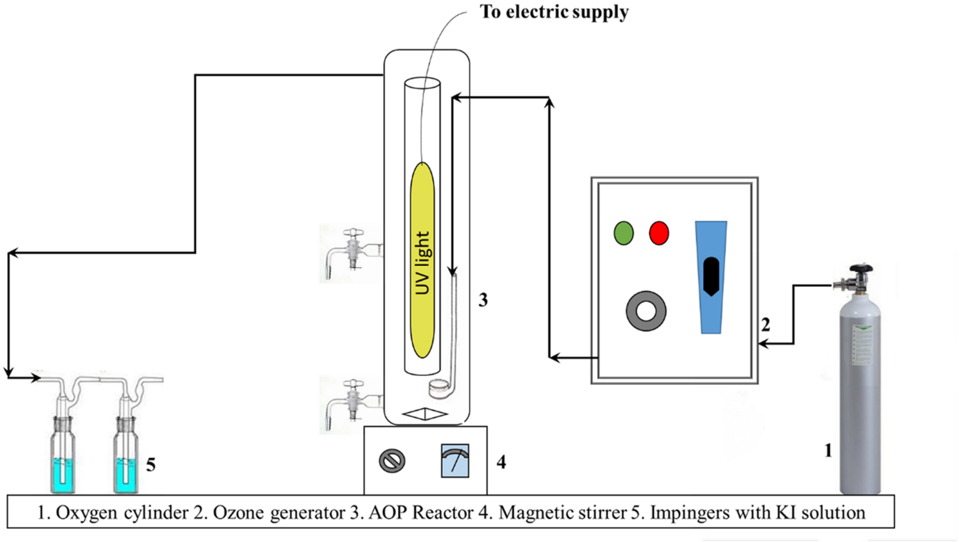

and 12, and pH was adjusted using sulfuric acid and caustic soda. The samples were collected at different time intervals and immediately quenched with 0.1 M $Na_2S_2O_3$ solution to remove the residual ozone. Then samples were filtered through Whatman filter paper and, after that, analyzed using a UV spectrophotometer. Finally, the unreacted gases are passed through a series of two potassium iodide bottles to trap the remaining ozone. All experiments were performed at room temperature only. The required quantity of persulphate and the prepared catalyst was added in $O_3$/UV/persulphate and $O_3$/catalyst process, respectively, by keeping all other experimental conditions the same. In $O_3$/UV process, A TUV G5 T5 model Philips 11 W lamp was used to conduct experiments using the same setup and experimental conditions. In the O3/catalyst process, the same procedure was followed to see the catalyst's reusability. After each run, the catalyst was separated, washed with distilled water, then dried and used in the next run. To see the degradation pathway, tert-butanol (TBA) as a radical scavenger was added by keeping all other experimental conditions the same. Finally, the collected samples were analyzed using a Shimadzu model TOC-V $_{\text{CPH/CPN}}$ supplied by Shimadzu Corporation, Japan.

### Characterization of catalyst

X-ray diffraction (XRD) was performed using an X-pert MPD system (Philips) using Cu-Kα radiation ($\lambda = 1.5406$ Å). Identification of crystal phases was carried out using JCPDS (Joint Committee on Powder Diffraction Standards) data bank. The detailed structure and morphology were analyzed using scanning electron microscope (SEM), and the elemental composition of the synthesized catalyst was analyzed by energy dispersive of X-ray (EDX) using a LEO 44i (JEOL) instrument. The surface area of synthesized catalyst was found using the nitrogen adsorption–desorption isotherms at – 195.126 °C using ASAP 2010 Micromeritics.

## Results and discussion

### Catalyst characterization

Catalyst morphology was determined by scanning electron microscopy (SEM) and depicted in Fig. 3a. As can be seen, the catalyst has a rod-like structure with a diameter in the nanometer range. Further, a sponge-like structure was also observed with pores in the nanometer range. Overall, it was observed that all the particles are agglomerated; however, the boundaries of different grains are visible for all samples. The micrograph reveals the uneven distribution of the different sizes of grains throughout the samples. The elemental composition of the metal in %wt for Ce–Co–O catalyst was determined by the EDS. The results are depicted in Fig. 3b. The EDS characterization confirms the presence of cerium, cobalt, oxygen, and carbon. The bimetallic catalyst Ce–Co–O prepared by the sol–gel method has 51 wt% of cobalt and 24.4 wt% cerium. The EDX results element composition of cerium, cobalt and oxygen in the catalyst is 26.07%, 40.55%, 26.81%, respectively.

The crystalline structure of catalyst Ce–Co–O was analyzed by the XRD method, and the result is depicted in Fig. 3c. The narrow peaks suggest that the catalyst is crystalline. The diffraction peaks at 2θ value of 15.41°, 34.58°, and 66.16° correspond to cerium oxide (Reference code-98-062-1709) and peaks at 20.14°, 23.99°, and 43.42° corresponding to cobalt oxide (Reference code-04-003-2613). The BET surface area, pore diameter, and pore volume of catalyst Ce–Co–O were determined by the nitrogen adsorption isotherms at – 195 °C. The surface area, pore

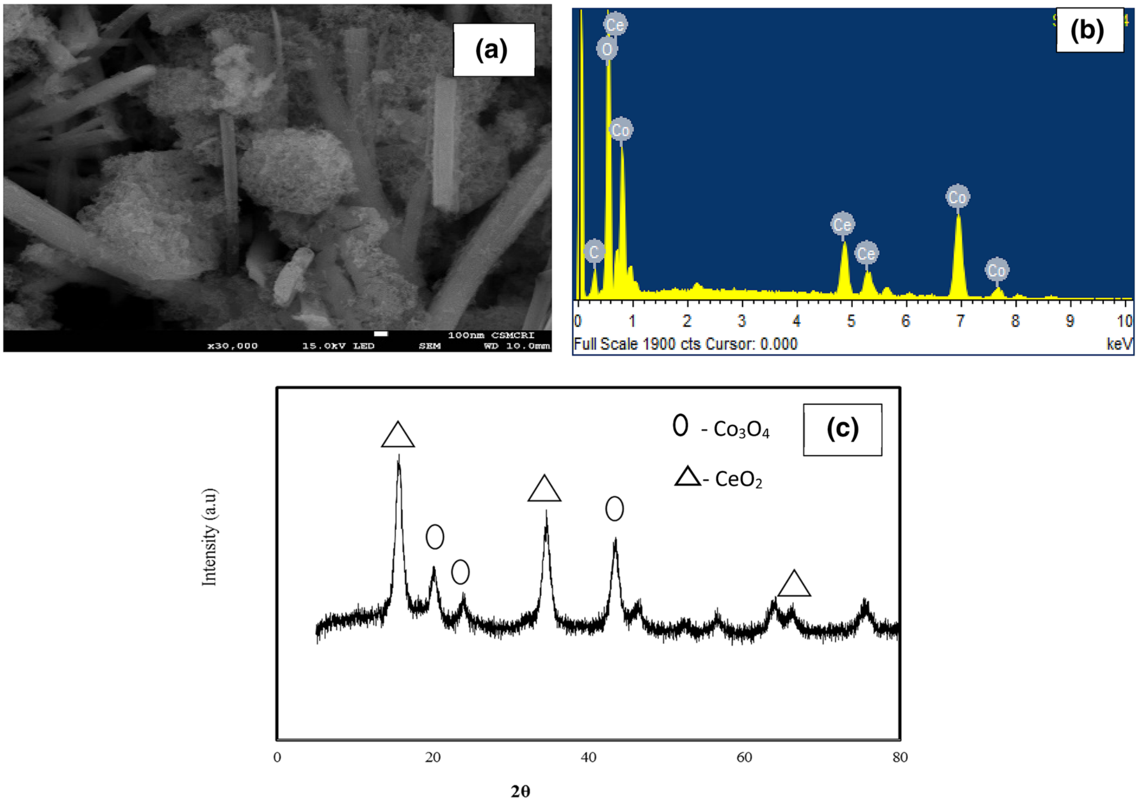

**Fig. 3** Characterization of synthesized catalyst Ce–Co–O **a** SEM micrograph **b** EDS spectrum **c** XRD pattern

diameter, and pore volume are 61.7987 $m^2/g$, 145.696 Å, 0.225095 $cm^3/g$, respectively. Beltran et al. [24] prepared the $Co_3O_4/Al_2O_3$ by impregnation method and reported the surface area was 128 $m^2/g$. Faria et al. [25] synthesized different catalyst Mn–O, Co–O, Ce–O, Ce–Mn–O and reported the surface area of 26 $m^2/g$, 29 $m^2/g$, 72 $m^2/g$, and 114 $m^2/g$, respectively. The high surface area ensures more active sites and high adsorption of pollutants, which facilitates the catalytic activities [4–6].

## Effect of applied ozone dose

Ozone dosage is one of the crucial parameters for the removal of RB5 dye, and it also affects the overall cost of the process [26]. As depicted in Fig. 4, the TOC removal efficiency increases with increase in the ozone flowrate.

The ozonation process results in 43.82% rise in TOC removal as the ozone flow rate increases from 30 to 60 LPH. Similar trends were observed in $O_3$/UV, $O_3$/UV/PS, and $O_3$/Cat processes. %TOC removal increases from 21.45%

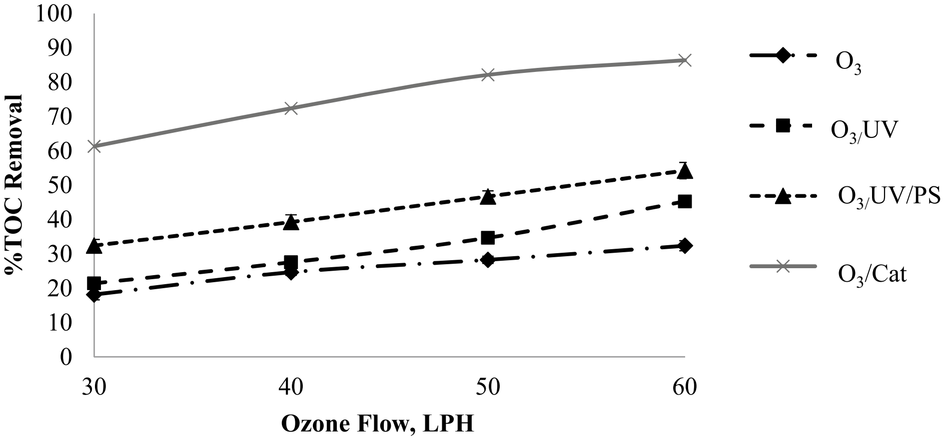

**Fig. 4** Effect of applied ozone dose on % TOC removal (process conditions: initial dye concentration 100 $mgL^{-1}$; pH 7; UV intensity 11 W; TOC: PS ratio 1:10; catalyst dosage: 0.5 g/L; reaction time 80 min)

to 45.30%, 32.45% to 54.27%, and 61.34% to 86.40% by employing $O_3$/UV, $O_3$/UV/PS, and $O_3$/Cat process, respectively. This improved efficiency could result from an increase in ozone flow rate, which accelerated the concentration of dissolved ozone in the reaction solution. This phenomenon helps in the decomposition of ozone and hence formes the more reactive species to remove RB5 [27]. The results are in good agreement with a reported study where CuO-$Cu_2O$/MCA was used to degrade textile dye effluent by catalytic ozonation process [28].

## Effect of initial pH

The efficiency of most AOPs is highly influenced by pH and is optimized at every time. Therefore, pH is one of the most important parameters that significantly affect the efficiency of AOPs and is always considered for optimization of the water treatment processes. Therefore, the effect of solution pH in the range of 2–12 was studied for all the ozone-based AOPs, and results are represented in Fig. 5.

As shown in Fig. 5, the ozonation process shows 69.47% higher TOC removal than at 2 pH. Ozonation process shows better results at higher pH as alkaline condition favors ozone decomposes into free radicals [29]. A similar pattern was observed in $O_3$/UV process, which shows 22.35%, 45.60%, and 58.45% TOC removal at pH 2, 7, and 12, respectively. $O_3$/UV/PS process results in 62.34% TOC removal at 12 pH, which is 54.21% higher than removal at 2 pH. The improvement in efficiency may be attributed to alkaline condition, which somewhat activates persulfate [21, 30, 31]. Additionally, sulfate radicals react with the hydroxide to form hydroxyl radical (OH●) in a highly alkaline medium [30]. In contrast, the O3/Cat process observed that the maximum RB5 removal was obtained at pH 7, 86.40%. The point of zero charges of synthesized catalyst was near 7.4. So, the catalyst surface would be positive for pH values less than 7.4 and negative for more than 7.4. Hence at pH lower than 7.4, there was an attraction between negative charge RB5 molecule and positive charge of the catalyst, which resulted in higher degradation efficiency [32, 33]. The higher removal at neutral pH suggests that the zero charges of the catalyst are more suitable in this system [34, 35].

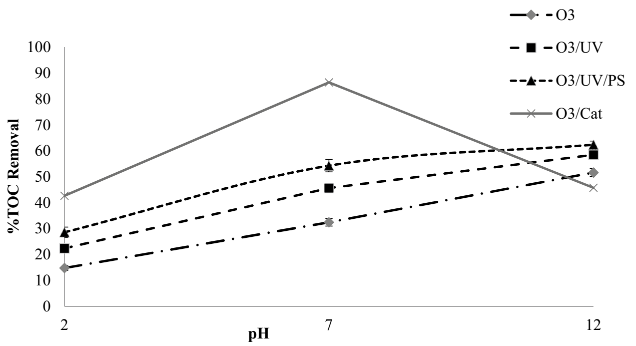

**Fig. 5** Effect of pH on % TOC removal (process conditions: initial dye concentration 100 $mgL^{-1}$; $O_3$ flowrate 60 LPH; pH 7; UV intensity 11 W; TOC: PS ratio 1:10; catalyst dosage: 0.5 g/L; reaction time 80 min)

## Effect of UV intensity

The ozonation coupled with UV radiation is an effective method for the degradation of recalcitrant pollutants [15]. $O_3$ and UV radiation enhance ozone decomposition by direct and indirect production of hydroxyl radicals which can mineralize numerous pollutants [36–38].

In the present study, the effect of UV light irradiation was studied by varying UV light by UV lamp power 11–66 W, and the results are shown in Fig. 6. It can be observed that with an increase in UV light intensity, TOC removal for RB5 was increasing. For example, in $O_3$/UV process, TOC removal was increased from 58.45 to 72.45% by increasing UV power from 11 to 66 W. A similar trend was observed in the O3/UV/PS process, which resulted in a 20.34% rise in TOC reduction as UV intensity increased from 11 to 66 W.

## Effect of persulfate dosage

Experiments were conducted to understand the role of persulfate in the removal of TOC in O3/UV/PS process. A couple of experiments were conducted at different TOC: PS ratios. Figure 7 depicts that RB5 degradation efficiency increased with increasing TOC: PS ratio from 1:10 to 1:60 while keeping other process variables constant.

The present study represents that maximum TOC removal was 90.32% at 1:40 TOC: PS ratio. After that, no substantial change in removal efficiencies was observed. Somewhat efficiency was decreased at a higher TOC: PS ratio. The decrease in efficiency may be due to the excess persulfate reacting with $SO_4^{\bullet-}$ and converting $SO_4^{\bullet}$ into

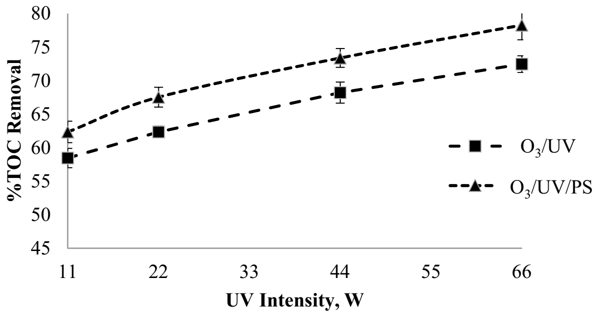

**Fig. 6** Effect of UV intensity on % TOC removal (process conditions: initial dye concentration 100 $mgL^{-1}$; $O_3$ flowrate 60 LPH; pH 12; TOC: PS ratio 1:10; reaction time: 80 min)

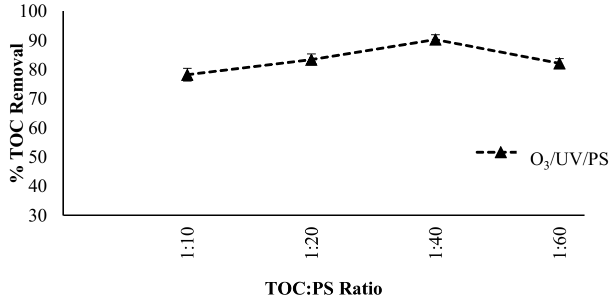

**Fig. 7** Effect of persulfate dosage on % TOC removal (process conditions: initial dye concentration 100 $mgL^{-1}$; $O_3$ flowrate 60 LPH; pH 12; UV intensity 66 W; reaction time 80 min)

sulfate ions [21, 39]. Furthermore, sulfate radicals may reach each other at higher concentrations and generate persulfate anions again [40].

## Effect of catalyst dosage

Catalyst dosage is also a very significant parameter in the heterogeneous system to optimize the usage of catalysts and minimize the operating cost of the process. The present study reveals that increasing the catalyst dosage has a positive effect on degradation efficiency.

Figure 8 represents that by increasing catalyst dosage from 0.5 to 1.0 $g/L^{-1}$, TOC removal increased from 86.34 to 96.28%. The increase in efficiency may be attributed to the simple reason that more catalyst provides more surface area, thus more surface area for direct mechanism and the hydroxyl radical generation [26]. In contrast, the excess amount of catalyst reduced performance. The reason could be that the particles are agglomerated and hence reduced surface area and the available active sites on the surface of catalyst (Ying Zhao 2020) [41].

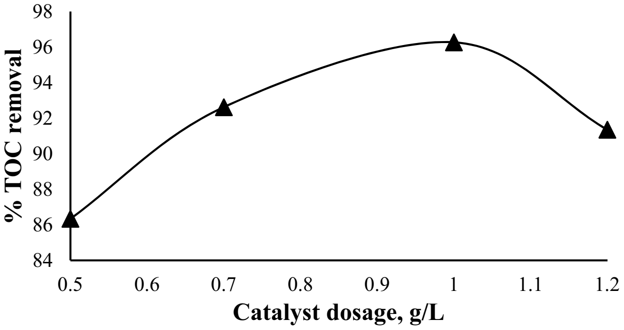

**Fig. 8** Effect of catalyst dosage on % TOC removal (process conditions: initial dye concentration 100 $mgL^{-1}$; $O_3$ flow 60 LPH; pH 7; reaction time 80 min)

## Effect of initial dye concentration

The efficiency of the AOPs for the degradation of organic pollutants is influenced by the process parameters, such as, the type of organic compound, pH, initial dye concentration, and temperature [42]. Further, the effect of initial RB5 concentration on its degradation efficiency was evaluated with the initial concentrations of 100, 300, 500, and 1000 $mgL^{-1}$, as shown in Fig. 9. The increase in initial RB5 concentration was found to reduce the degradation efficiency.

In the ozonation process, TOC removal was 51.60% at 100 mg/L of initial dye concentration, and it was reduced to 21.48% at 1000 mg/L of dye concentration. A similar trend was observed in all ozone-based AOPs taken into study. In addition, %TOC removal was reduced to 53.37%, 58.51%, and 55.05% in $O_3$/UV, $O_3$/UV/PS, and $O_3$/Cat process, respectively, by increasing RB5 dye concentration from 100 to 1000 mg/L. The probable reason for this is that as dye concentration increased, more intermediates resulted due to the degradation of parent dye. Thus the available ozone is utilized to degrade parent dye plus the intermediated formed due to the degradation (Kaoutar El Hassani 2019) [43].

## Conclusion

Ozone-based advanced oxidation processes are efficient and reliable options for wastewater treatment compared to conventional treatment methods. The main focus of this study was to remove the RB5 by employing ozone-based AOPs and compare the same. The different operating parameters were studied and compared in terms of the TOC removal efficiency. Among these, the best performance was observed

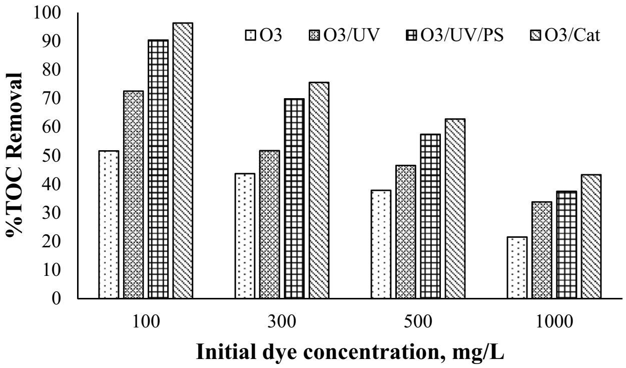

**Fig. 9** Effect of initial concentration of dye on % TOC removal in presence of employed AOPs {process conditions for $O_3$, $O_3$/UV and $O_3$/UV/PS: $O_3$ flow: 60 LPH; pH:12; UV intensity: 66 W; TOC:PS ratio: 1:40 (only for $O_3$/UV/PS); reaction time: 80 min} {process conditions for $O_3$/Cat: $O_3$ flow: 60 LPH; pH:7; Cat: 1 $g/L^{-1}$; reaction time: 80 min}

in the $O_3$/catalyst process, which resulted in 96% TOC removal at optimum operating parameters 60 LPH ozone flowrate, 7 pH, 100 mg/L RB5 concentration, and 1 g/L catalyst dosage in 80 min of reaction time. However, $O_3$/UV/PS resulted 90% TOC removal at ozone flowrate 60 LPH, 12 pH, 100 mg/L RB5 concentration, UV intensity 66 W and TOC/PS ratio 1:40 in 80 min of reaction time. Therefore, combined ozone-based AOPs were found to be an alternative method for wastewater treatment and thus may have the potential to solve the major environmental issue of degradation of recalcitrant or refractory, or non-biodegradable COD.

**Acknowledgements** The authors would like to thank Nirma University, Ahmedabad, Gujarat, for providing all necessary help and support to carry out the research work.

**Funding** Not applicable.

**Data availability** All data generated or analyzed during this study are included in this article.

## Declarations

**Conflict of interest** The authors declare that they have no known competing financial interests or personal relationships that could have appeared to influence the work reported in this paper.

**Consent for publication** Authors give copyrights to the journal as per the rules.

## References

1. Jose A, Lara-Ramos S-G, Daniel V-R, Jennyfer D-A, Mueses M, Machuca-Martínez F (2019) Intensification of the O3/TiO2/UV advanced oxidation process using a modified flotation cell. Photochem Photobiol Sci 18:920–928. https://doi.org/10.1039/C8PP00308D
2. Ambaye TG, Hagos K (2020) Photocatalytic and biological oxidation treatment of real textile wastewater. Nanotechnol Environ Eng 5(3):1–11
3. Baruah M, Supong A, Bhomick PC, Karmaker R, Pongener C, Sinha D (2020) Batch sorption–photodegradation of Alizarin Red S using synthesized TiO 2/activated carbon nanocomposite: an experimental study and computer modelling. Nanotechnol Environ Eng. https://doi.org/10.1007/s41204-020-00071-3
4. Dhiman P, Kumar A, Shekh M, Sharma G, Rana G, Vo DVN, ALOthman ZA (2021) Robust magnetic ZnO-Fe2O3 Z-scheme hetereojunctions with in-built metal-redox for high performance photo-degradation of sulfamethoxazole and electrochemical dopamine detection. Environ Res 197:111074
5. Dhiman P, Rana G, Kumar A, Sharma G, Vo DVN, AlGarni TS, ALOthman ZA (2021) Nanostructured magnetic inverse spinel Ni-Zn ferrite as environmental friendly visible light driven photodegradation of levofloxacin. Chem Eng Res Des. https://doi.org/10.1016/j.cherd.2021.08.028
6. Dhiman P, Patial M, Kumar A, Alam M, Naushad M, Sharma G, Kumar R (2021) Environmental friendly and robust Mg0.5-xCuxZn0.5Fe2O4 spinel nanoparticles for visible light driven degradation of Carbamazepine: band shift driven by dopants. Mater Lett 284:129005
7. Kumar J, Bansal A (2015) CFD simulations of immobilized-titanium dioxide based annular photocatalytic reactor: Model development and experimental validation. Indian J Chem Technol 22:95–104
8. Ratan JK, Saini A (2019) Enhancement of photocatalytic activity of self-cleaning cement. Mater Lett 244:178–181
9. Saini A, Arora I, Ratan JK (2020) Photo-induced hydrophilicity of microsized-TiO2 based self-cleaning cement. Mater Lett 260:126888
10. Zhou X, Meng M, Sun Z, Li Q, Jiang Z (2011) Prominent enhancement of Mn or Co addition on the performance of Cu-Ce-O catalyst used for H2 production via dimethyl ether steam reforming. Chem Eng J 174:400–407. https://doi.org/10.1016/j.cej.2011.09.018
11. Zhang N, Li JM, Liu GG, Chen XL, Jiang K (2017) Photodegradation of diclofenac in seawater by simulated sunlight irradiation: the comprehensive effect of nitrate, Fe(III) and chloride. Mar Pollut Bull 117(1–2):386–391. https://doi.org/10.1016/j.marpolbul.2017.02.024
12. Zhou X, Meng M, Sun Z, Li Q, Jiang Z (2011) Prominent enhancement of Mn or Co addition on the performance of Cu-Ce-O catalyst used for H2 production via dimethyl ether steam reforming. Chem Eng J 174(1):400–407
13. Mecha AC, Onyango MS, Ochieng A, Fourie CJS, Momba MNB (2016) Synergistic effect of UV–vis and solar photocatalytic ozonation on the degradation of phenol in municipal wastewater: a comparative study. J Catal 341:116–125. https://doi.org/10.1016/j.jcat.2016.06.015
14. Parrino F, Camera-Roda G, Loddo V, Palmisano G, Augugliaro V (2014) Combination of ozonation and photocatalysis for purification of aqueous effluents containing formic acid as probe pollutant and bromide ion. Water Res 50:189–199. https://doi.org/10.1016/j.watres.2013.12.001
15. Hussain M, Mahtab MS, Farooqi IH (2020) The applications of ozone-based advanced oxidation processes for wastewater treatment: a review. Adv Environ Res 9(3):191–214. https://doi.org/10.12989/aer.2020.9.3.191
16. Amr A, Salem S, Aziz HA, Adlan MN, Bashir MJK (2013) Pretreatment of stabilized leachate using ozone/persulfate oxidation process. Chem Eng J 221:492–499. https://doi.org/10.1016/j.cej.2013.02.038
17. Hilles AH, AbyAmr SS, Alkarkhi AFM, Hossain MS (2019) The effect of persulfate oxidation on the biodegradability of concentrated anaerobic stabilized leachate. Sains Malays 48(11):2381–2390. https://doi.org/10.17576/jsm-2019-4811-09
18. Soubh A, Mokhtarani N (2016) The post treatment of composting leachate with a combination of ozone and persulfate oxidation processes. RSC Adv 80:76113–76122. https://doi.org/10.1039/C6RA09539A
19. Cao J, Zhang W-X, Brown DG, Sethi D (2008) Oxidation of lindane with Fe(II)-activated sodium persulfate. Environ Eng Sci 25(2):221–228. https://doi.org/10.1089/ees.2006.0244
20. Lin Y-T, Liang C, Chen J-H (2011) Feasibility study of ultraviolet activated persulfate oxidation of phenol. Chemosphere 82(8):1168–1172. https://doi.org/10.1016/j.chemosphere.2010.12.027
21. Soubh AM, Baghdadi M, Abdoli MA, Aminzadeh B (2018) Activation of persulfate using an industrial iron-rich sludge as an efficient nanocatalyst for landfill leachate treatment. Catalysts 8:218. https://doi.org/10.3390/catal8050218
22. Li P, Miao R, Wang P, Sun F, Li X-Y (2021) Bi-metal oxide-modified flat-sheet ceramic membranes for catalytic ozonation of organic pollutants in wastewater treatment. Chem Eng J. https://doi.org/10.1016/j.cej.2021.131263

23. Guo L, Xiao Z, Sun W, Hao Xu, Yanhua Xu, Zheng H, Sun Y (2021) Fischer–Tropsch synthetic wastewater treatment with Fe/Mn@CH: catalytic ozonation and process evaluation. Sep Purif Technol 276:119274. https://doi.org/10.1016/j.seppur.2021.119274
24. Beltran FJ, Rivas FJ, Montero-de-Espinosa R (2003) Ozone-enhanced oxidation of oxalic acid in water with cobalt catalysts. 2. Heterogeneous catalytic ozonation. Ind Eng Chem Res 42:3218–3224
25. Faria PCC, Monteiro DCM, Órfão JJM, Pereira MFR (2009) Cerium, manganese and cobalt oxides as catalysts for the ozonation of selected organic compounds. Chemosphere 74:818–824. https://doi.org/10.1016/j.chemosphere.2008.10.016
26. Ghuge SP, Saroha AK (2018) Catalytic ozonation for the treatment of synthetic and industrial effluents—application of mesoporous materials: a review. J Environ Manag 211:83–102. https://doi.org/10.1016/j.jenvman.2018.01.052
27. Zhang H, He Y, Lai L, Yao G, Lai Bo (2020) Catalytic ozonation of Bisphenol A in aqueous solution by Fe3O4–MnO2 magnetic composites: performance, transformation pathways and mechanism. Sep Purif Technol 245:116449. https://doi.org/10.1016/j.seppur.2019.116449
28. Hu E, Wu X, Shang S, Tao X-M, Jiang S-X, Gan L (2016) Catalytic ozonation of simulated textile dyeing wastewater using mesoporous carbon aerogel supported copper oxide catalyst. J Clean Prod 112:4710–4718. https://doi.org/10.1016/j.jclepro.2015.06.127
29. Cuerda-Correa EM, Alexandre-Franco MF, Fernández-González C (2020) Advanced oxidation processes for the removal of antibiotics from water. An overview. Water. https://doi.org/10.3390/w12010102
30. Furman OS, Teel AMYL, Watts RJ (2010) Mechanism of base activation of persulfate. Environ Sci Technol 44:6423–6428. https://doi.org/10.1021/es1013714
31. Liang C, Guo YY (2012) Remediation of diesel-contaminated soils using persulfate under alkaline condition. Water Air Soil Pollut 223:4605–4614. https://doi.org/10.1007/s11270-012-1221-6
32. Wong CPP, Lai CW, Lee KM, Hamid SBA (2015) Advanced chemical reduction of reduced graphene oxide and its photocatalytic activity in degrading reactive black 5. Material 8(10):7118–7128. https://doi.org/10.3390/ma8105363
33. Chokshi NP, Patel D, Atkotiya R, Ruparelia J (2020a) Catalytic ozonation of Reactive Black 5 in aqueous solution over a La-Co-O catalyst. J Indian Chem Soc 97:373–378
34. Zhu H, Ma W, Han H, Han Y, Ma W (2017) Catalytic ozonation of quinoline using nano-MgO: efficacy, pathways, mechanisms and its application to real biologically pretreated coalgasification wastewater. Chem Eng J. https://doi.org/10.1016/j.cej.2017.06.025
35. Ren Y, Dong Q, Feng J, Ma J, Wen Q, Zhang M (2012) Magnetic porous ferrospinel NiFe2O4: a novel ozonation catalyst with strongcatalytic property for degradation of di-n-butyl phthalate and convenientseparation from water. J Colloid Interface Sci 382:90–96. https://doi.org/10.1016/j.jcis.2012.05.053
36. Lovato ME, Gilliard MB, Cassano AE, Martín CA (2014) Kinetics of the degradation of n-butyl benzyl phthalate using O3/UV, direct photolysis, direct ozonation and UVeffects. Environ Sci Pollut Res. https://doi.org/10.1007/s11356-014-2796-9
37. Paucar NE, Kim I, Tanaka H, Sato C (2019) Effect of O3 dose on the O3/UV treatment process for the removal of pharmaceuticals and personal care products in secondary effluent. ChemEngineering. https://doi.org/10.3390/chemengineering3020053
38. Rekhate CV, Srivastava JK (2020) Recent advances in ozone-based advanced oxidation processes for treatment of wastewater: a review. Chem Eng J Adv 3:100031. https://doi.org/10.1016/j.ceja.2020.100031
39. Yang S, Yang X, Shao X, Niu R, Wang L (2011) Activated carbon catalyzed persulfate oxidation of Azo dye acid orange 7 at ambient temperature. J Hazard Mater 186:659–666. https://doi.org/10.1016/j.jhazmat.2010.11.057
40. Deng J, Shao Y, Gao N, Deng Y, Tan C, Zhou S (2014) Zero-valent iron/persulfate(Fe0/PS) oxidation acetaminophen in water. Int J Environ Sci Technol 11:881–890. https://doi.org/10.1007/s13762-013-0284-2
41. Chokshi NP, Ruparelia JP (2021) Synthesis of nano Ag-La-Co composite metal oxide for degradation of RB 5 dye using catalytic ozonation process. Ozone Sci Eng. https://doi.org/10.1080/01919512.2021.1901070
42. Ali F, Khan JA, Shah NS, Sayed M, Khan HM (2018) Carbamazepine degradation by UV and UV-assisted AOPs: kinetics, mechanism and toxicity investigations. Process Saf Environ Prot 117:307–314. https://doi.org/10.1016/j.psep.2018.05.004
43. Chokshi NP, Ruparelia JP (2020b) Catalytic ozonation of Reactive Black 5 over silver-cobalt composite oxide catalyst. J Inst Eng India Ser A 101:433–443. https://doi.org/10.1007/s40030-020-00454-4
44. Mena E, Rey A, Beltrán FJ (2018) TiO2 photocatalytic oxidation of a mixture of emerging contaminants: a kinetic study independent of radiation absorption based on thedirect-indirect model. Chem Eng J 339:369–380. https://doi.org/10.1016/j.cej.2018.01.122
45. Lara-Ramos JA, Saez C, Machuca-Martínez F, Rodrigo MA (2020) Electro-ozonizers: a new approach for an old problem. Sep Purif Technol 241:116701. https://doi.org/10.1016/j.seppur.2020.116701
46. Liu Z, Demeestere K, Van Hulle S (2021) Comparison and performance assessment of ozone-based AOPs in view of trace organic contaminants abatement in water and wastewater: a review. J Environ Chem Eng 9:105599. https://doi.org/10.1016/j.jece.2021.105599